Available online at www.sciencedirect.com
SCIENCE DIRECT®
Analytica Chimica Acta 507 (2004) 87–93
ANALYTICA CHIMICA ACTA
www.elsevier.com/locate/aca

Peak tailing in electrophoresis due to alteration of the wall charge by adsorbed analytes a Numerical simulations and asymptotic theory

Karim Shariff [a], Sandip Ghosal [b,*]

[a] *NASA Ames Research Center, Moffett Field, CA 94305, USA*
[b] *Mechanical Engineering, Northwestern University, Evanston, IL 60208, USA*

Received 6 June 2003; received in revised form 3 October 2003; accepted 16 October 2003

Abstract

When analytes containing cationic components, such as proteins, are separated in fused silica capillaries or micro-chips, they adsorb strongly to the negatively charged channel walls. Broadened and highly asymmetric peaks in the detector signal is symptomatic of the presence of such wall interactions. Band broadening is caused by the introduction of shear into the electroosmotic flow which leads to Taylor dispersion. The shearing flow in turn is caused by axial variations in zeta-potential due to adsorbed analytes. In this paper, numerical solutions of the coupled electro-hydrodynamic equations for fluid flow and the advection-diffusion equation for analyte concentration are presented in the limit of thin Debye layers. The simulations reproduce many of the qualitative effects of wall adsorption familiar from observation. Further, the simulation results are compared, and found to agree very well (to within a percent for characteristic values of the parameters) with a recently developed asymptotic theory.

PACS: 47.70.-n; 47.70.Fw; 47.85.-g

Keywords: Capillary zone electrophoresis; Dispersion; Wall interactions

1. Introduction

The tendency of proteins and peptides to adsorb to the silica walls of micro-channels is a serious impediment to achieving acceptable resolution in separations [1–5] using capillary zone electrophoresis (CZE) either in cylindrical capillaries or in microchannels etched on chips. A large effort has been invested in designing wall coatings and buffer additives that will reduce or eliminate analyte-wall interactions [6]. Such treatments are effective in many cases though no universal solution has been found to date covering all relevant applications. The remedies often introduce further difficulties such as suppression of the electroosmotic flow (EOF), issues of stability and reproducibility of the coatings and possible contamination of the sample [6]. The subject of this paper is the analysis and quantitative prediction of band broadening in CZE due to adsorption of analytes to capillary walls. In this paper, we assume a circular cross-section for the micro-channel, however the qualitative effects are equally valid for channels of other cross-sectional shapes such as those on microfluidic chips.

An obvious deleterious effect of analyte adsorption at capillary walls is that some of the sample is lost from the fluid stream. The adsorbed analyte may be difficult to wash off and if it is a protein, it may denature on the capillary surface perhaps ruining the capillary (or the chip). Analyte adsorption leads to reduced signal levels, strongly assymetric (tailed) peaks and reduced resolution due to the following sequence of events which has only recently been fully understood [7–9]. When a charged species adsorbs to the capillary wall it alters the surface charge on the wall and therefore the zeta-potential. Thus, as the analyte plug traverses the capillary it causes the zeta potential to vary in the axial direction and also to vary in time. The well known formula for electroosmotic flow speed, $u_e = -\epsilon\zeta E/4\pi\mu$ (where ϵ and μ are the dielectric constant and viscosity of the buffer, E is the

* Corresponding author. Tel.: +1-847-4675990; fax: +1-847-4913915.
E-mail address: s-ghosal@northwestern.edu (S. Ghosal).

0003-2670/$ – see front matter © 2003 Elsevier B.V. All rights reserved.
doi:10.1016/j.aca.2003.10.052

applied electric field and ζ is the local ζ potential) would then imply that different cross-sections of the capillary will have different fluid fluxes, a scenario incompatible with the fact that liquids are incompressible. The apparent paradox is resolved through the appearance of induced pressure gradients in the axial direction that enforce the incompressibility condition, even though no external pressure difference may have been applied across the capillary. The actual electroosmotic flow is intermediate in character between electroosmotic flow in a capillary with uniform ζ-potential and a pressure driven flow. Since pressure driven flows have a parabolic rather than a uniform profile, the altered electroosmotic flow is no longer uniform over the capillary cross-section. The resulting enhanced "Taylor dispersion" or "shear induced dispersion" [10,11] is what causes the band broadening and peak tailing observed in the CZE signal.

In this paper, the governing equations describing electroosmotic flow and analyte dispersion in a cylindrical capillary in the presence of wall interactions are formulated (Section 2) and solved numerically (Section 3) in the limit of infinitely thin Debye layers and Stokes flow. The numerical solution is compared (Section 4) with the result of a recently developed asymptotic theory (Appendix A). Conclusions are summarized in Section 5.

2. Mathematical formulation

We consider CZE in a cylindrical capillary of length L_0 and radius a_0. In the absence of analyte adsorption and in the limit of thin Debye layers, the electroosmotic flow speed in such a capillary is (in cgs units)

$$u_e = -\frac{\epsilon\zeta_0 E}{4\pi\mu} \tag{1}$$

where ϵ is the dielectric constant of the fluid, E the applied electric field, μ the viscosity and ζ_0 is the wall ζ-potential (in the absence of wall interactions). The variables of interest are the concentration of the sample in the fluid, $\tilde{c}(\tilde{r}, \tilde{x}, \tilde{t})$ (moles per unit volume) and adsorbed to the wall, $\tilde{s}(\tilde{x}, \tilde{t})$ (moles per unit area), the ζ-potential $\tilde{\zeta}(\tilde{x}, \tilde{t})$, the fluid flow velocity $\tilde{\boldsymbol{u}}(\tilde{r}, \tilde{x}, \tilde{t})$ and the fluid pressure $\tilde{p}(\tilde{r}, \tilde{x}, \tilde{t})$ which depend on the distance from the axis of the capillary, $\tilde{r}$, distance from the inlet, $\tilde{x}$, and the time, $\tilde{t}$. For each such variable, $\tilde{f}$, we will define a dimensionless counterpart $f = \tilde{f}/f_*$ where f_* is a characteristic value for the variable $\tilde{f}$. We choose the following characteristic values $x_* = r_* = a_0$, $t_* = a_0/u_e$, $u_* = u_e$, $\zeta_* = \zeta_0$, $c_* = c_{max}$, $p_* = \mu u_e/a_0$ and $s_* = a_0 c_{max}$. Here, $\sim c_{max}$ is the maximum value of c at the initial time. In the following we will only work with the dimensionless variables f and will seldom refer to the dimensional counterparts $\tilde{f}$ again.

The evolution of c is governed by an advection-diffusion equation:

$$\frac{\partial c}{\partial t} + \nabla\cdot[(\boldsymbol{u} + u_{ep}\hat{\boldsymbol{x}})c] = Pe^{-1}\nabla^2 c, \tag{2}$$

where $Pe = u_e a_0/D$ (the Peclet number), D being the molecular diffusivity; u_{ep} is the electrophoretic speed in units of u_e. For definiteness, we consider only a single species and set $u_{ep} = 0$, since the only effect of u_{ep} is a uniform translation of the peak relative to the mean flow. The Reynolds number is Re (where ν is the kinematic viscosity of the fluid) $= (a_0 u_e)/\nu$. In microfluidic applications typically $Re \sim 0.01$–1. For small Reynolds number, the electroosmotic flow is governed by the Stokes form of the hydrodynamic equations:

$$-\nabla p + \nabla^2\boldsymbol{u} = 0, \tag{3}$$

$$\nabla\cdot\boldsymbol{u} = 0. \tag{4}$$

with the coupling to the electric field E provided by the Helmholtz-Smoluchowski slip boundary condition [12]

$$u(1, x, t) = \zeta(x, t). \tag{5}$$

If analytes with net molecular charge are adsorbed on the surface, the density of surface charges and hence the surface ζ-potential is altered. We take this effect into account through the relation

$$\zeta(x, t) = 1 - \alpha s(x, t), \tag{6}$$

where α is a dimensionless parameter. We shall regard α as a given constant that may either be determined from theory (a linearization of Gouy–Chapman theory, for instance) or by experiment. The interaction of the analyte with the wall is modeled by a Langmuir second order kinetic law [13]

$$\frac{\partial s}{\partial t} = k_a c_w(x, t)[s_{max} - s(x, t)] - k_d s(x, t), \tag{7}$$

where k_a and k_d are (dimensionless) rates of adsorption and desorption, respectively, and $c_w(x, t) = c(1, x, t)$ is the analyte concentration evaluated at the wall. The term with s_{max} expresses the fact that there are a finite number of charged sites at the wall where analyte can be adsorbed and hence the wall has a saturation point. The dimensionless parameters characterizing the interaction with the wall can be readily related to the corresponding dimensional parameters; $s_{max} = \tilde{s}_{max}/(a_0 c_{max})$, $k_a = (c_{max} a_0/u_e)\tilde{k}_a$, $k_d = (a_0/u_e)\tilde{k}_d$ and $\alpha = -(a_0 c_{max}/\zeta_0)(\partial\tilde{\zeta}/\partial\tilde{s})$. Since Eq. (7) must match the diffusive flux of $c(r, x, t)$ at the wall

$$\frac{\partial s}{\partial t} = -Pe^{-1}\left(\frac{\partial c}{\partial r}\right)_{r=1}. \tag{8}$$

3. Numerical method

The characteristic length of a CZE capillary, $L_0 \sim$ 10–100 cm but a characteristic radius is $a_0 \sim$ 10–100 μm. Since the computational grid size is determined by the smallest relevant length scale in the problem (in this case the grid size must be chosen to achieve proper resolution in the r-direction) the simulation of the above problem

is numerically intensive (or "stiff") for realistic values of $L = L_0/a_0 = 10^3$ to 10^5.

The size of the computational problem can be reduced by exploiting an exact solution for electroosmotic flow in a cylindrical capillary due to Anderson and Idol [14]. This solution assumes

(1) Stokes flow ($Re = 0$).
(2) Helmholtz–Smoluchowski slip boundary conditions for infinitely thin Debye layers, Eq. (5).
(3) Axial symmetry, so that the ζ-potential is a function of x and t only, $\zeta = \zeta(x, t)$.

Under those assumptions, the velocity field $\boldsymbol{u} = u\hat{\boldsymbol{x}} + \hat{\boldsymbol{r}}v$ may be expressed in terms of the stream function ψ,

$$u = -\frac{1}{r}\frac{\partial \psi}{\partial r} \tag{9}$$

$$v = \frac{1}{r}\frac{\partial \psi}{\partial x} \tag{10}$$

where the stream function is given by a series expansion

$$\psi = -\frac{r^2}{2}\langle\zeta\rangle + 2\sum_{m=1}^{\infty} a_m^{\mathrm{c}}(r)\cos\left(\frac{2m\pi x}{L}\right) + 2\sum_{m=1}^{\infty} a_m^{\mathrm{s}}(r)\sin\left(\frac{2m\pi x}{L}\right) \tag{11}$$

where

$$\frac{a_m^{\mathrm{c}}}{\hat{\zeta}_m^{\mathrm{c}}} = \frac{a_m^{\mathrm{s}}}{\hat{\zeta}_m^{\mathrm{s}}} = \frac{rI_0(\alpha_{\mathrm{m}})I_1(\alpha_{\mathrm{m}}r) - r^2 I_0(\alpha_{\mathrm{m}}r)I_1(\alpha_{\mathrm{m}})}{\alpha_{\mathrm{m}}I_1^2(\alpha_{\mathrm{m}}) + 2I_0(\alpha_{\mathrm{m}})I_1(\alpha_{\mathrm{m}}) - \alpha_{\mathrm{m}}I_0^2(\alpha_{\mathrm{m}})} \tag{12}$$

and

$$\hat{\zeta}_m^{\mathrm{c}} = \frac{1}{L}\int_0^L \zeta(x, t)\cos\left(\frac{2m\pi x}{L}\right)\mathrm{d}x \tag{13}$$

$$\hat{\zeta}_m^{\mathrm{s}} = \frac{1}{L}\int_0^L \zeta(x, t)\sin\left(\frac{2m\pi x}{L}\right)\mathrm{d}x \tag{14}$$

are the cosine and sine transform of the ζ function, $\zeta(x, t)$, at the time instant for which the flow is being determined, $\alpha_m = 2m\pi/L$, and $\langle\cdot\rangle$ indicates the average over the length of the capillary:

$$\langle\zeta\rangle = \frac{1}{L}\int_0^L \zeta\,\mathrm{d}x. \tag{15}$$

In Eq. (12), I_n denotes the modified Bessel function of integer order n.

Thus, only the advection-diffusion problem Eq. (2) and Eq. (7) with boundary condition Eq. (8) needs to be solved numerically. The velocity field $\boldsymbol{u}$ appearing in Eq. (2) is obtained at each time step from the Anderson and Idol analytical result presented above. The latter depends on $\zeta(x, t)$ which in turn is related to $s(x, t)$ through Eq. (6). The adsorbed concentration $s(x, t)$ is obtained by evolving $s(x, t)$ according to Eq. (7). Thus, the problem reduces to solving a pair of coupled partial differential equations for $c(r, x, t)$ and $s(x, t)$ with given initial and boundary conditions. For initial condition we will choose

$$c(r, x, 0) = c_0(x) \tag{16}$$

$$s(x, 0) = 0 \tag{17}$$

where c_0 will be some specified function centered at x_0 and having some characteristic width σ_0. The parameters x_0 and σ_0 are chosen so that the initial concentration profile is localized near the inlet but with negligible concentration at $x = 0$. Physically this corresponds to a short time after injection of the sample plug.

For boundary conditions in the x-direction we shall use 'periodic' boundary conditions, $c(r, 0, t) = c(r, L, t)$. This is an artifice that is commonly used when (a) the true inlet and exit boundary conditions are not known (b) the system is not very sensitive to conditions at these boundaries. Indeed, mathematically the 'periodic' boundary conditions correspond to replacing the problem of a single analyte plug travelling through a single capillary of finite length by an infinite array of such capillaries joined end to end each containing an analyte plug. However, if during the time period under study, the concentration remains essentially zero at the two ends, then the result of computing with the periodic boundary condition differs only very slightly from a calculation that uses more 'natural' boundary conditions such as $c(r, 0, t) = 0$ and $c(r, L, t) = 0$. The periodic boundary condition has the advantage of allowing a Fourier decomposition of the concentration field which permits the use of highly accurate spectral methods. One must be careful though in ensuring that the concentration peak is kept well clear of either boundary during the course of the simulation, since otherwise one would obtain the unrealistic situation of the sample re-entering at the inlet end upon exiting the opposite end of the capillary. In the simulation the initial concentration peak is centered sufficiently far from the inlet end so that the concentration at the inlet is negligible, and, the simulation is stopped before the sample gets too close to the outlet so that no significant concentration builds up at the outlet during the time period represented in the simulation.

A finite volume approach [15] is adopted for the numerical solution of Eq. (2). This approach has the advantage that any conservation laws that the continuum equations satisfy are also satisfied exactly in the spatially discretized system. This is important in order to avoid a "spurious decay" of the peak due to numerical effects. For example, Eq. (2) together with boundary condition (8) and the periodic boundary condition in x imply that

$$\frac{\mathrm{d}}{\mathrm{d}t}\left[\int_0^L \mathrm{d}x\int_0^1 2\pi r c(r, x, t)\mathrm{d}r + \int_0^L 2\pi s(x, t)\,\mathrm{d}x\right] = 0 \tag{18}$$

which express the fact that the the total number of molecules (whether in solution or adsorbed to the wall) of the sample

remains constant. In the absence of time discretization errors a finite volume approach guarantees the validity of the corresponding discrete relation

$$\frac{\mathrm{d}}{\mathrm{d}t}\left[\sum_j\sum_k 2\pi r_k c_{j,k}\Delta r_k \Delta x_j + \sum_j 2\pi s_j \Delta x_j\right] = 0 \qquad (19)$$

where Δr_k and Δx_j are grid spacings in the radial and axial directions and the indices 'j' and 'k' label the grid points.

For simplicity all spatial derivatives are approximated by second-order finite differences. Time integration is performed using the fourth-order Runge–Kutta scheme with time increments chosen to fulfil the CFL (Courant-Friedrichs-Levy) condition. The simulations were performed with 2521 points in the axial direction and 20 points in the radial direction. A finer grid led to no visible change in the results which suggests a converged calculation.

4. Results

The following estimates (to within an order of magnitude) may be made for typical CZE systems: capillary radius $a_0 \sim 50\,\mu\mathrm{m}$, capillary length $L_0 \sim 0.5\,\mathrm{m}$, viscosity (water) $\nu \approx 10^{-6}\,\mathrm{m^2/s}$, diffusivity $D \sim 10^{-9}\,\mathrm{m^2/s}$ (for small to moderate sized molecules) and typical electroosmotic flow speed $u_\mathrm{e} \sim 10^{-3}\,\mathrm{m/s}$. This allows us to make the following estimates $Re \sim 0.05$ and $Pe \sim 50$. The remaining dimensionless parameters k_a, k_d, s_max and α that characterize the wall interactions are more difficult to estimate since to the best of the authors' knowledge there appears to be no published data on these parameters for interactions of cationic proteins with fused silica walls. If the source of the attraction to the wall is primarily electrostatic in origin, then it is reasonable to suppose that saturation ($s = s_\mathrm{max}$) corresponds to neutralization of the wall charge ($\zeta = 0$). This requires $\alpha = 1/s_\mathrm{max}$ so we will choose the parameter α in this way. Experiments by Towns and Regnier [16] show that the fraction of sample that is adsorbed varies within wide limits from zero to essentially hundred percent (no signal recovered). However, the interesting parameter regime to study is the situation where the fraction adsorbed ~ 0.5. If the fraction adsorbed is very much less than this, wall interactions are a relatively weak effect and if it is much larger then no signal is likely to be detected so that the calculation is irrelevant. In order to determine the k_a that would achieve this, let us for the purpose of making a very rough estimate assume that the sample consists of a homogeneous cylindrical plug of fixed length σ_*. Then, neglecting desorption and assuming that the walls are far from saturation, we can write the following equation for the time evolution of the concentration of our sample in the cylinder: $\pi a_0^2 \sigma_* (\mathrm{d}\tilde{c}/\mathrm{d}\tilde{t}) = -(2\pi a_0 \sigma_*)\tilde{k}_\mathrm{a}\tilde{s}_\mathrm{max}\tilde{c}$. Therefore, after time $\tilde{t} \sim L_0/u_\mathrm{e}$ taken to traverse the capillary, the remaining concentration may be estimated as $\tilde{c} \sim c_\mathrm{max}\exp[-2L_0\tilde{k}_\mathrm{a}\tilde{s}_\mathrm{max}/(a_0 u_\mathrm{e})]$. For $\tilde{c}/c_\mathrm{max} \sim 0.5$, we must have $L_0\tilde{k}_\mathrm{a}\tilde{s}_\mathrm{max}/(a_0 u_\mathrm{e}) \sim 1$ or in terms of dimensionless variables, $Lk_\mathrm{a}s_\mathrm{max} \sim 1$. Clearly, for k_d, there is no lower limit on what can be considered as an 'interesting regime'. Indeed, for relatively large proteins, k_d is essentially zero [6]. However, an upper bound on 'reasonable values' for k_d may be estimated. To do so, note that if k_d is large, s is essentially zero ahead and behind the plug and at the plug, the adsorption and desorption processes must be practically at equilibrium. Thus, equating the right hand side of (7) to zero we have

$$s \approx \frac{s_m}{1 + (k_\mathrm{d}/k_\mathrm{a})c_\mathrm{w}^{-1}} \approx \left(\frac{k_\mathrm{a}}{k_\mathrm{d}}\right) s_m \qquad (20)$$

since $c_\mathrm{w} \approx 1$. Thus, if $k_\mathrm{d} \gg k_\mathrm{a}$, $s \ll s_m$ in which case the modification of the zeta-potential is unimportant. Thus the parameter regime of interest to us, is $0 < k_\mathrm{d} \simeq k_\mathrm{a}$. The parameters for the numerical simulation, displayed in Table 1, were chosen so as to be consistent with the above estimates for typical systems. Other parameter values do not make a significant difference to the main qualitative results, and need not be reported here (see e.g. [9]).

Table 1
Parameter Values for Simulation

Parameter	L	Re	Pe	α	k_a	k_d	s_max
Value	1000	0	100	$1/s_\mathrm{max}$	0.1	0.0005	0.01

The initial conditions chosen for the numerical simulation were $s(x, 0) = 0$ (so that $\zeta(x, 0) = 1$) and $c(r, x, 0) = c_0(x)$ where $c_0(x)$ had the trapezoidal shape shown in Fig. 1. The asymptotic theory requires only initial values of s and $\bar{c}$ to be specified (henceforth, an overbar denotes average over the cross-section, $\bar{c} = \int_0^1 2rc\,\mathrm{d}r$). The radial distribution of c is then determined by Eq. (A.1) in Appendix A. For the asymptotic theory we assumed $s(x, 0) = 0$ and $\bar{c}(x, 0) = c_0(x)$. Note however that this implies a slight radial dependence of the concentration profile given by (A.1), so that the initial conditions for the simulation and the asymptotic theory are not quite identical even though the concentration

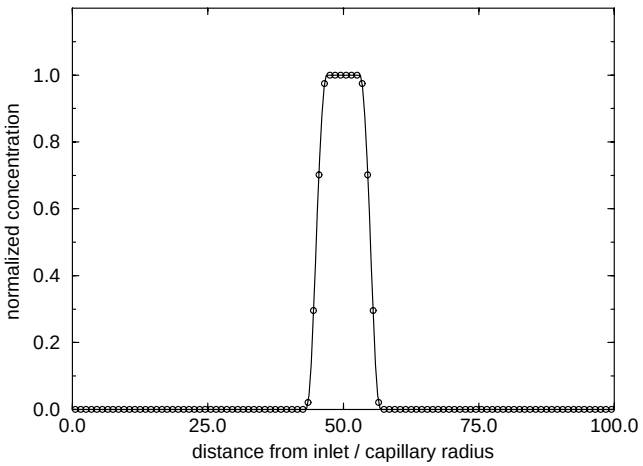

Fig. 1. Initial analyte concentration profile $c_0(x)$; symbols: asymptotic theory, line: numerical simulation.

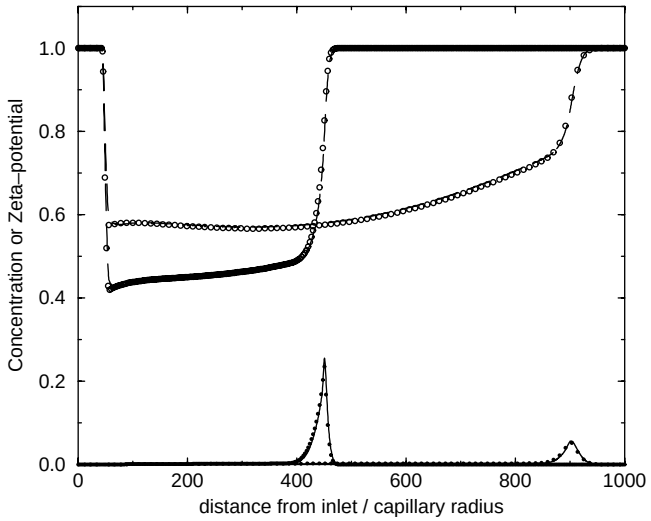

Fig. 2. Comparison of asymptotic theory (symbols) with numerical simulation (lines) of the cross-sectionally averaged analyte concentration (lower curves) and ζ-potential (upper curves) at two time instants. The initial concentration is shown in Fig. 1.

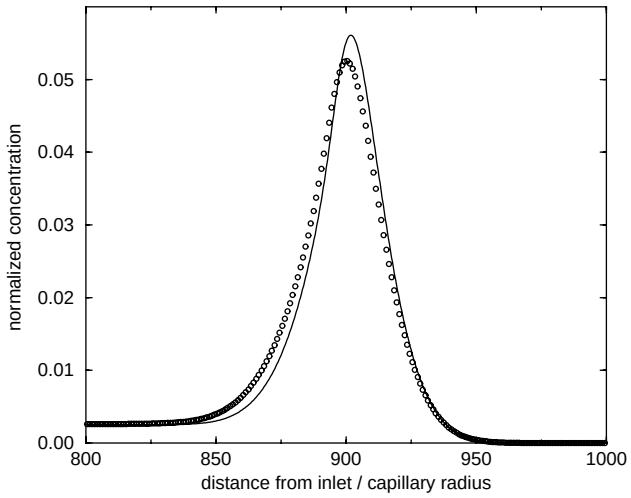

Fig. 3. Same as Fig. 2 but showing only the concentration profile at the second downstream station on a magnified scale.

averaged over the cross-section are the same. However the difference represents a fast decaying transient and as the detailed comparisons presented in the remainder of this section will show, the slight mismatch in initial conditions does not have any significant effect on the quantities of interest. If desired this mismatch could be eliminated by substituting $\bar{c} = c_0$ in (A.1) and using the resulting function $c(r, x, t)$ as the proper initial condition for the numerical simulation.

Fig. 2 shows the distribution of $\bar{c}$ and ζ at the instant when the concentration peak arrives at a hypothetical detector placed at a distance x_d from the inlet. The figure shows two sets of results for $x_d = 450$ and $x_d = 900$ respectively. These graphs refer to the spatial distribution of $\bar{c}$ and ζ for a single analyte species at two different instants of time and should not be confused with multiple peaks from a multicomponent sample. It is seen that as the sample moves down the capillary, the peak height decreases, the peak width increases and the peak shape becomes markedly asymmetric. The peak shapes have a striking similarity with observed CZE signals in an uncoated capillary for cationic proteins (see e.g. Fig. 8 of [16] and Fig. 10 of [17]; in making the comparison one should keep in mind that in the detector signals the horizontal axis represents time of arrival at a fixed detector location so that the sharp edge appears first, and then the gradually decaying tail). The following rationalization of the asymmetric peak seems plausible: Taylor dispersion by itself is known, in the long time limit, to lead to a Gaussian profile of the concentration. Thus, a thin slab of fluid either ahead or behind the centroid of the distribution would contain the same amount of analyte provided the distance from the centroid is the same in both cases. However, the slab behind the centroid has most of the material distributed on the outer periphery whereas the slab ahead of the centroid would have most of the material near the centerline. Therefore wall adsorption is more effective at removing material from the slab behind the centroid, which would cause an assymetric shape in the profile. Desorption does not play a significant role in the peak asymmetry as the effect persists even for $k_d = 0$ [9].

As expected, the ζ-potential is seen to be reduced behind the analyte peak. However, with passage of time, the ζ-potential at a fixed position undergoes a gradual recovery. This is due to desorption from the capillary walls. For a short section near the inlet, $\zeta = 1$ because in the simulation the sample is introduced at $x = 50$ rather than at $x = 0$ in order to ensure that the concentration at the inlet remains essentially zero throughout the simulation. For both $\bar{c}$ and ζ the simulation is seen to be in excellent agreement with the theoretical calculation using the 1D Eq. (A.3) presented in Appendix A. Fig. 3 shows an amplified view of the second peak (at detector $x_d = 900$). The difference between the asymptotic theory and the exact solution is seen to be small. Note that in Fig. 3 the concentration does not drop to zero after passage of the peak, but there is a "plateau" extending many diameters behind the peak. Such "lack of return to the baseline" is well known in the presence of wall interactions. It is usually attributed to irreversible adsorption of analyte to the detection window, however the presence of this plateau in the concentration profile could also be a contributing factor. This long plateau is caused by the cumulative effect of the analyte desorbing from the wall long after the main peak has passed.

Fig. 4 shows the arrival time as a function of distance from the inlet for the sample peak. Such 'elution time delays' due to protein adsorption and its underlying causes are now well understood [7,16]. Even though on the basis of formal analysis we expect the asymptotic theory to be accurate only after a 'transition length' of the order of the Peclet number (100) times the capillary radius, it is seen that in practice, no significant error is made if it is used throughout the capillary.

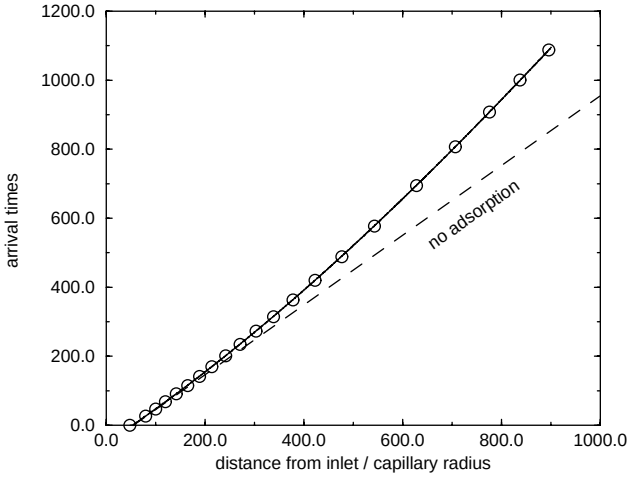

Fig. 4. Comparison of asymptotic theory (symbol) with simulation (solid line) for arrival time of concentration peak as a function of the distance to the observation point from the inlet. The dashed line gives the elution times in the absence of wall interactions.

5. Conclusion

The problem of the elution of a sample plug by electroosmotic flow in the presence of wall interactions was numerically simulated using a set of characteristic parameters typical of the separation of cationic proteins in fused silica capillaries. The adsorption of the sample to the wall and its subsequent desorption was modeled using Langmuir second order kinetics. The adsorption of solute from the fluid stream was assumed to change the ζ-potential in a linear fashion, which in turn affected the hydrodynamics. The Debye layer thickness was assumed very thin compared to the capillary radius so that the coupling between electrical effects and hydrodynamics could be modeled using the Helmholtz-Smoluchowski slip boundary conditions. The hydrodynamics itself was considered in the Stokes flow limit, which allowed the use of an exact analytical formula due to Anderson and Idol for calculating the velocity field at each time instant. The partial differential equation for the sample concentration was integrated using a finite volume method using the velocity fields determined from Anderson and Idol's formula.

The numerical simulation was used to test the validity of a recently developed asymptotic theory due to Ghosal [9] that reduces the solution of the problem to that of solving a pair of coupled partial differential equations for $\bar{c}(x, t)$ and $s(x, t)$ in one space dimension. The theory is expected to be accurate at distances from the inlet $\tilde{x} \gg a_0 Pe$ where a_0 is the capillary radius and Pe is the Peclet number defined earlier. Naturally, for the theory to be useful the total capillary length, L_0 must satisfy $L_0 \gg a_0 Pe$. The agreement between the computed result and the asymptotic theory was found to be extremely good. The fact that the theory is not expected to be very accurate over a short transition length $a_0 Pe > \tilde{x} > 0$, was found not to have a significant impact on the accuracy of the solution at later times.

The computation reproduced many of the well known qualitative effects of wall interaction in CZE. Significant peak broadening, peak tailing and reduction in peak intensity was observed. Peak shapes consistent with observed shapes in the presence of strong wall interactions were found. In the presence of desorption, the main peak was found to be followed by a very long low level 'plateau' due to the delayed arrival of slowly desorbing analytes. This phenomenon too is supported by practical observations.

Numerical simulation is a useful tool for the analytical chemist as it provides the ability to calculate performance parameters for microfluidic devices. For example, if a certain wall coating has been designed that reduced adsorption by a known factor one could calculate what effect this will have on the plate count. If the change in the adsorption/desorption coefficients with repeated use is modeled suitably, one could calculate how the resolution of the separation device might degrade over time. The problem size for a direct numerical simulation of the whole system is generally very large on account of the small aspect ratio between the capillary radius and length. The reduced set of one dimensional equations discussed here provides a much more efficient way of accomplishing such calculations with very little reduction in the accuracy of the results.

Acknowledgements

This research was conducted at the NASA Ames Research Center in the summer of 2002 during which one of us (S.G.) was supported by the NASA-ASEE-SJSU Faculty Fellowship Program (NFFP).

Appendix A. Asymptotic theory for sample concentration

The principal results of the asymptotic theory presented in [9] is summarized below in the special case where (a) $Re \to 0$, (b) a single species interacts with the wall.

Following the same notation as in the rest of the paper, the sample concentration is given by

$$c(r, x, t) = \bar{c}(x, t) + \tfrac{1}{4} Pe(1 - 2r^2)\partial_t s + \tfrac{1}{24} Pe(2 - 6r^2 + 3r^4)(\zeta - \bar{u})\partial_x \bar{c}. \quad \text{(A.1)}$$

The zeta-potential is related to s by Eq. (6) and, if the flow is driven purely by a potential drop (that is no pressure drop is imposed), then

$$\bar{u} = \langle \zeta \rangle \quad \text{(A.2)}$$

where $\langle \cdot \rangle$ denotes average over the length of the capillary as defined in (15). Thus, c is "slaved" to $\bar{c}$ and s the dynamics

of which evolve on a slow (compared to the molecular diffusion time across the capillary in the radial direction) time scale.

The slow dynamics is described by the following evolution equations

$$\frac{\partial \bar{c}}{\partial t} + (\bar{u} + u_{\mathrm{ep}})\frac{\partial \bar{c}}{\partial x} = \frac{\partial}{\partial x}\left(D_{\mathrm{eff}}\frac{\partial \bar{c}}{\partial x}\right) + S \tag{A.3}$$

where

$$D_{\mathrm{eff}} = \frac{1}{Pe} + \frac{Pe}{48}(\zeta - \bar{u})^2, \tag{A.4}$$

is an "effective" diffusivity and

$$S = -2\frac{\partial s}{\partial t} + \frac{Pe}{12}\frac{\partial}{\partial x}\left[(\zeta - \bar{u})\frac{\partial s}{\partial t}\right], \tag{A.5}$$

is a source term that is reponsible for the removal of analyte from the buffer. Finally, s evolves according to

$$\begin{aligned}\frac{\partial s}{\partial t} &= f(\bar{c}, s) - \tfrac{1}{4}Pe\ f\partial_{c_{\mathrm{w}}} f\big|_{c_{\mathrm{w}}=\bar{c}} \\ &\quad -\tfrac{1}{24}Pe(\zeta - \bar{u})\partial_x \bar{c}\ \partial_{c_{\mathrm{w}}} f\big|_{c_{\mathrm{w}}=\bar{c}}\end{aligned} \tag{A.6}$$

where $f(c_{\mathrm{w}}, s)$ denotes the function on the right hand side of (7).

References

[1] R. Weinberger, Practical Capillary Electrophoresis, Academic Press, New York, 2000.
[2] J. Jorgenson, New Directions in Electrophoretic Methods, American Chemical Society, 1987 (Chapter 1).
[3] J. Jorgenson, New Directions in Electrophoretic Methods, American Chemical Society, 1987 (Chapter 13).
[4] J. Landers (Ed.), Introduction to Capillary Electrophoresis, CRC Press, Boca Raton, FL, 1996.
[5] P. Camilleri (Ed.), Capillary Electrophoresis, Theory and Practice, CRC Press, Boca Raton, FL, 1998.
[6] E. Doherty, R. Meagher, M. Albarghouthi, A. Barron, Electrophoresis 24 (2003) 34–54.
[7] S. Ghosal, Anal. Chem. 74 (2002) 771–775.
[8] S. Ghosal, J. Fluid Mech. 459 (2002) 103–128.
[9] S. Ghosal, J. Fluid Mech. 419 (2003) 285–300.
[10] G. Taylor, Proc. R. Soc. A 219 (1953) 186–203.
[11] R. Aris, Proc. R. Soc. A 235 (1956) 67–77.
[12] R. Probstein, Physicochemical Hydrodynamics, Wiley, New York, 1994.
[13] B. Gaš, M. Štědrý, A. Rizzi, E. Kendler, Electrophoresis 6 (1995) 958–967.
[14] J. Anderson, W. Idol, Chem. Eng. Commun. 38 (1985) 93–106.
[15] H. Lomax, T. Pulliam, D. Zingg, Fundamentals of Computational Fluid Dynamics, Springer, Berlin, 2001.
[16] J. Towns, F. Regnier, Anal. Chem. 64 (1992) 2473–2478.
[17] G. Bruin, R. Huisden, J. Kraak, H. Poppe, J. Chromatogr. 480 (1989) 339–349.